The Journal of Veterinary Medical Science

FULL PAPER

Physiology

L-amino acid oxidase-1 is involved in the gut-liver axis by regulating 5-aminolevulinic acid production in mice

Mohammad Ibrahim QASIMI[1)], Susumu FUKUZAWA[1)], Ken SUENAGA[1)], Jun KAMBE[1)], Chunmei LI[2)], Shozo TOMONAGA[3)], Takahiro KAWASE[4)], Takamitsu TSUKAHARA[4)], Kazuhiko HIRAYAMA[5)], Ryo INOUE[6)], Yuki YAMAMOTO[1)], Kentaro NAGAOKA[1)]*

[1)]Laboratory of Veterinary Physiology, Department of Veterinary Medicine, Tokyo University of Agriculture and Technology, Tokyo, Japan
[2)]College of Animal Science and Technology, Nanjing Agricultural University, Nanjing, China
[3)]Division of Applied Biosciences, Graduate School of Agriculture, Kyoto University, Kyoto, Japan
[4)]Kyoto Institute of Nutrition and Pathology, Kyoto, Japan
[5)]Laboratory of Public Health, Department of Veterinary Medicine, The University of Tokyo, Tokyo, Japan
[6)]Laboratory of Animal Science, Department of Applied Biological Science, Setsunan University, Osaka, Japan

ABSTRACT. L-amino acid oxidase (LAAO) is a metabolic enzyme that converts L-amino acids into ketoacids, ammonia, and hydrogen peroxide (H_2O_2). The generated H_2O_2 has previously been shown to have antibacterial and gut microbiota-modulatory properties in *LAO1* knock-out (KO) mice. Since most microbial metabolites reach the liver through the portal vein, we examined gut-liver interactions in *LAO1* KO mice. We found lower total cholesterol levels, higher glutamic pyruvic transaminase (GPT) levels in the serum, and higher pro-inflammatory cytokine mRNA expression in the liver tissue. In wild-type (WT) mice, LAO1 was expressed in gut tissues (ileum and colon). Microbiome analysis revealed that the abundance of some bacteria was altered in *LAO1* KO mice. However, short-chain fatty acid (SCFAs) levels in cecal feces and gut permeability did not change. Fecal microbiota transplantation (FMT) revealed that feces from *LAO1* KO mice slightly stimulated pro-inflammatory cytokine expression in the liver. During metabolomic analysis, 5-aminolevulinic acid (5-ALA) was the only metabolite found to be significantly upregulated in the portal and abdominal veins of the *LAO1* KO mice. Intraperitoneal administration of 5-ALA to WT mice significantly increased IL-6 mRNA expression in the liver. These observations suggest that gut LAO1 plays a role in regulating 5-ALA production and that a high level of 5-ALA stimulates the liver to increase pro-inflammatory cytokine expression by disrupting LAO1 in mice.

KEYWORDS: 5-aminolevulinic acid, gut microbiota, L-amino acid oxidase-1, liver

J. Vet. Med. Sci.
85(6): 672–679, 2023
doi: 10.1292/jvms.23-0080

Received: 13 February 2023
Accepted: 17 April 2023
Advanced Epub:
3 May 2023

Given that the liver receives most of its blood supply (nearly 70%) from the gut through the portal vein, it serves as the first organ exposed to gut-derived products in addition to bacteria and their derivatives [4, 9]. Generally, under healthy conditions, the detoxification ability of the liver and gut barrier functions are essential for an active defense mechanism [17]. However, gut leakage induction and bacterial translocation enable microbial metabolites to reach the liver, impairing the capacity to process bile acids and promoting gut dysmotility and inflammatory processes. These conditions can lead to gut dysbiosis and aggravate liver damage. Studies on the interaction between gut microbiota and the liver are necessary to understand the pathophysiology of various liver diseases [5, 17].

A flavoenzyme called L-amino acid oxidase (LAAO) catalyzes the oxidative deamination of L-amino acids and produces the corresponding keto acids, ammonia, and H_2O_2 [18, 23]. LAAO exhibits distinct properties and excellent bioactivity in various animals [14]. The main components that fight invading germs and exhibit antibacterial action are H_2O_2 generated by the oxidation of L-amino acid substrates, mainly phenylalanine, methionine, and tyrosine [14, 24]. In mammals, the genes L-amino acid oxidase-1 (*LAO1*) and interleukin 4-induced gene 1 (*IL4i1*) are linked to two similar molecules [21]. *LAO1* knockout (KO) mice show learning and memory

*Correspondence to: Nagaoka K: nagaokak@cc.tuat.ac.jp, Laboratory of Veterinary Physiology, Department of Veterinary Medicine, Tokyo University of Agriculture and Technology, 3-5-8 Saiwai-cho, Fuchu-shi, Tokyo 183-8509, Japan
(Supplementary material: refer to PMC https://www.ncbi.nlm.nih.gov/pmc/journals/2350/)

failure due to impaired amino acid metabolism in the brain [24]. In addition, mice lacking the *LAO1* gene showed an altered gut microbiota composition; that is, the gut microbiota of lactating *LAO1* KO pups was highly diverse in their feces, whereas those of the wild-type (WT) were composed of only a few dominant bacteria, such as *Lactobacillus* spp [23]. It is unknown whether gut microbiota diversity is maintained during adulthood and whether the diversity of the gut microbiota in *LAO1* KO mice affects liver function.

Since disturbance in gut-liver access is potentially the leading cause of several liver diseases, this study aimed to investigate liver function, gut microbiota composition, and serum metabolites in adult *LAO1* KO mice. We found that mice lacking the *LAO1* gene showed higher glutamic pyruvic transaminase (GPT) concentrations in blood, higher pro-inflammatory cytokine expression in the liver, changes in the gut microbiota, and higher 5-ALA levels in the portal and abdominal veins. To determine the potential mechanism, we performed fecal microbiota transplantation (FMT) in germ-free mice and intraperitoneally injection of 5-ALA into WT mice.

MATERIALS AND METHODS

Animals and sample collection

LAO1 KO mice backcrossed with C57BL/6 mice were maintained as previously described [18]. The mice were kept in cages containing wood-shaving bedding at 23 ± 2°C under a 14 hr lighting schedule (lights on 05:00 to 19:00) with free access to food (MR-Breeder, Nosan Corp., Yokohama, Kanagawa, Japan) and tap water. Blood, feces, and tissues were collected from fully 12 weeks old anesthetized mice. The blood was centrifuged at 3,000 rpm for 15 min, and the plasma was stored at −20°C until use. Cecal feces were collected and weighed to determine the composition of the microbiota and short-chain fatty acids (SCFAs). For gene expression analysis, the liver, ileum, and colon tissues were cut into small pieces and snap-frozen. The remaining tissue was fixed in 4% paraformaldehyde for histological examination.

Germ-free (GF) BALB/cA male mice were maintained at 24 ± 1°C under a 12 hr lighting schedule with *ad libitum* access to food and water at The University of Tokyo. For FMT, rectal feces samples were collected from WT and *LAO1* KO mice and maintained under anaerobic conditions until use. Each feces were diluted 100 times (w/v) by trypticase soy broth without dextrose (pH 7.2), which was anaerobic in advance, and added Na_2CO_3 0.84 g/L, Bacto Agar 0.5 g/L and L-Cysteine 0.5 g/L. The diluted solutions were administered to the GF mice (0.5 mL) by oral gavage using a feeding needle. Liver tissue was collected four weeks after FMT.

All procedures were approved by the Institutional Animal Care and Use Ethics Committee of the Tokyo University of Agriculture and Technology (Approval number 23-1, R03-110) and The University of Tokyo (approval number: P15-132).

Measurements of plasma biochemical parameters

The blood plasma of *LAO1* KO and WT mice was analyzed for glucose (Glu) and total cholesterol (T-Cho) concentrations using the glucose CII-test (FUJIFILM Wako Pure Chemical Corp., Osaka, Japan) and cholesterol E-test (FUJIFILM Wako Pure Chemical Corp.). Glutamic oxaloacetic transaminase (GOT) and glutamate pyruvate transaminase (GPT) plasma levels were determined using a Transaminase CII-test kit (FUJIFILM Wako Pure Chemical Corp.). All procedures were performed according to the manufacturer's instructions.

Real-time PCR

Total RNA was extracted from liver and gut samples using ISOGEN II Reagent (Nippon Gene Co., Ltd., Tokyo, Japan), and cDNA was synthesized using a PrimeScript II first-strand cDNA synthesis kit (Takara Bio Inc., Kusatsu, Japan) according to the manufacturer's instructions. The Primer3 program was used to create oligonucleotide primers for real-time PCR (Supplementary Table 1). PCR was performed using PowerUp SYBER Green Master Mix (Thermo Fisher Scientific, Waltham, MA, USA). The expression of target mRNA relative to α-tubulin mRNA was determined using the $2^{-\Delta\Delta}$CT method.

Immunofluorescence analysis

Specimens were deparaffinized and subjected to antigen retrieval by boiling for 15 min in 0.01 M sodium citrate buffer (pH 6.0). The slides were blocked with 2% BSA/PBS for one hour, treated with anti-LAO1 [18] for one hour, and incubated with Alexa 647 conjugated anti-rabbit IgG (Thermo Fisher Scientific) for one hour. The slides were mounted using ProLong Gold with DAPI (Thermo Fisher Scientific). Images were captured using an immunofluorescence microscope (BZ-X700an, Keyence, Osaka, Japan).

DNA extraction from feces

Microbial genomic DNA was extracted from feces collected from the cecum using the QuickGene DNA Tissue Kit S (FUJIFILM Wako) according to the manufacturer's instructions. Briefly, 40 mg of feces, 15 mg of 0.2 mm glass beads (No. 02, Toshin Riko, Co., Ltd., Tokyo, Japan), and 200 µL of tissue lysis buffer were mixed, and beads were homogenized at 3,000 rpm for 120 sec using a Micro Smash Cell Disrupter (MS-100, Tomy Seiko Co., Ltd., Tokyo, Japan). Proteinase K (25 µL) was added to the homogenized sample and incubated at 55°C for 1 hr. The sample was then centrifuged for 10 min at 16,000 × *g* and 20°C, and the supernatant was transferred to another microtube containing 180 µL of lysis buffer and incubated at 70°C for 10 min. Following incubation, 240 µL of 99% ethanol was added to the microtube and vortexed for 15 sec. The lysate was transferred to a QuickGene Mini 480 cartridge and pressurized. A washing buffer (750 µL) was added to the cartridge thrice. After the third wash, elution buffer (200 µL) was added, and the mixture was incubated at 20°C. DNA was extracted after the third pressurization. The DNA concentration was adjusted to 20 ng/µL using an elution buffer.

Library preparation and DNA sequencing

The 16S rRNA metagenomic analysis was performed as described previously [13]. Briefly, the first PCR targeting variable regions 3 and 4 (V3–4) of the 16S rRNA gene was performed using primers 341F (CCT ACG GGN GGC WGG AG) and 805R (GAC TAC HVG GGT ATC TAA TCC), followed by a second PCR to attach the dual indices. The amplicons from the second PCR were purified, and the concentration was normalized using the SequalPrep Normalization Plate Kit (Life Technologies, Tokyo, Japan). The size and quantity of the library were assessed using a Bioanalyzer 2100 (Agilent Technologies Japan, Tokyo, Japan) and Library Quantification Kit for Illumina (Kapa Biosciences), respectively. The library was mixed with the phiX control and sequenced using a MiSeq v3 kit (Illumina Inc., San Diego, CA, USA) according to the manufacturer's instructions. The sequence data were processed using QIIME2 (ver. 2021.11), and the imported reads were denoised using the DADA2 plugin to generate the ASV feature table. Singletons and ASVs assigned to the mitochondria and chloroplasts were excluded from further analysis. Taxonomy was assigned to the filtered ASVs using a pre-trained QIIME2-compatible SILVA version 138 database (99% full-length sequences). The microbial variance was assayed using the MicrobiomeAnalyst software with default settings (https://www.microbiomeanalyst.ca).

Measurement of SCFAs

SCFA concentrations in the mice feces were analyzed using a gas chromatography-mass spectrometry apparatus (GCMS-QP2010 Ultra, Shimadzu, Kyoto, Japan) equipped with an autosampler (AOC 5000, Shimadzu), as previously described with minor modifications [15]. Briefly, 300 mg of individual mouse feces was diluted with 0.6 mL distilled water. Later, the diluents were mixed with 12% pericolic acid (v/v) (90 µL), centrifuged at 13,000 × *g* for 10 min at 4°C, and the supernatants were filtered through 0.45 µm cellulose acetate membrane filter and degassed under vacuum. The supernatant (5 µL) was injected into an SIL-10 autoinjector (Shimadzu). SCFAs were separated using two serial organic acid columns (Shim-pack SCR-102H, Shimadzu) with an isocratic delivery pump (LC-10ADvp; Shimadzu) and an online degasser (DGU-12A; Shimadzu) and quantified using a system controller (CBM-20A; Shimadzu).

Untargeted metabolomic analysis

A total of 50 µL plasma, 5 µL of 1 mg/mL 2-Isopropylmalic acid as internal standard, and 250 µL of MeOH/H_2O/$CHCl_3$ (5:2:2, v/v/v) were mixed and incubated with shaking at 1,200 rpm for 30 min at 37°C. The samples were centrifuged at 16,000 × *g* for 5 min at 4°C, and 225 µL of the supernatant was collected and evaporated in a vacuum concentrator centrifuge at RT for 20 min. After evaporation, the samples were freeze-dried overnight at RT. For derivatization, 40 µL of pyridine containing 20 mg/mL of methoxyamine hydrochloride was added to the freeze-dried samples, mixed, and incubated with shaking at 1,200 rpm for 90 min at 30°C. Subsequently, N-methyl-N-trimethylsilyltrifluoroacetamide (20 µL) was added, mixed, and incubated with shaking at 1,200 rpm for 45 min at 37°C. The samples were then used for GC-MS analysis. Gas chromatography-mass spectrometry (GC-MS) was performed using a GCMS-QP2010 Ultra instrument (Shimadzu). Low-molecular-weight metabolites were identified using a commercially available SHIMADZU GC/MS Metabolite Database Ver.2 (Shimadzu), and data analysis was conducted using MetaboAnalyst (https://www.metaboanalyst.ca/,) [3].

Gut permeability analysis

Water starvation was performed on the mice one day before treatment. Fluorescein isothiocyanate-conjugated dextran (FITC-dextran) (molecular weight: 4,000) (Sigma-Aldrich Co., St. Louis, MO, USA) was dissolved in PBS at a concentration of 20 mg/mL and orally administered through a feeding needle attached to a 1 mL syringe (500 g/mouse). After 4 hr post-gavage, blood samples were collected from the mice and centrifuged at 3,000 rpm for 10 min. Using diluted FITC-dextran (0, 125, 250, 500, 1,000, 2,000, 4,000, 6,000, and 8,000 ng/mL) in PBS as standard, the fluorescence intensity in each plasma was measured by Wallac 1420 ARVOsx (PerkinElmer, Inc., Waltham, MA, USA).

Administration of 5-ALA

Recently, 5-ALA has received much attention as a therapeutic agent [8, 11] and feed additive [10]. Metabolomic analysis revealed that 5-ALA levels were significantly higher in the portal and abdominal veins of LAO1 KO mice. Consequently, we focused our efforts on understanding 5-ALA and its effects on the liver. Two experiments were conducted using WT animals to understand the effects of this chemical on liver function. For the low-dose experiment, 10 mice were injected daily with saline or 40 mg/kg BW 5-ALA hydrochloride (Fujifilm Wako Pure Chemical Corp., Osaka, Japan) for one week. The other high-dose experiment involved IP injection of a higher dose of 5-ALA (100 mg/kg BW) or saline every three days for ten days. The doses used in this study were selected based on the therapeutic doses previously used in mice. After sacrificing the mice under general anesthesia, the samples were collected.

Statistical analysis

Data were analyzed and visualized using MicrobiomeAnalyst, MetaboAnalyst, and GraphPad Prism 9 software (GraphPad Software, San Diego, CA, USA). The plasma biochemical parameters, gene expression, SCFAs, IgA, and FITC-dextran were statistically compared using Student's *t*-test. Differences were considered statistically significant at $P<0.05$.

RESULTS

Body weight, plasma, and liver parameters

No significant difference was observed in the body and liver weight between *LAO1* KO and WT mice (Fig. 1A). Furthermore, the

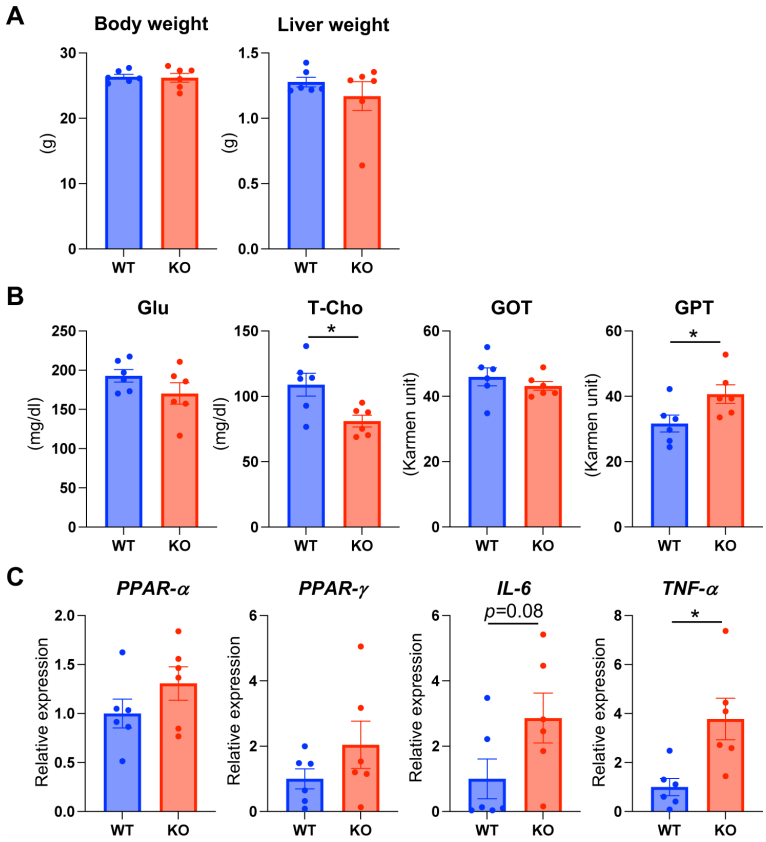

Fig.1. Body weight, plasma, and liver parameters. The mean of body and liver weights (**A**), and glucose [Glu], total cholesterol [T-Cho], glutamic-oxaloacetic aminotransferase [GOT], glutamic-pyruvic aminotransferase [GPT] levels in plasma (**B**); and *PPAR-α*, *PPAR-γ, interleukin-6* [*IL-6*], and *tumor necrosis factor-α* [*TNF-α*] mRNA expression in the liver of WT and *LAO1* KO mice (**C**). * Indicated $P<0.05$.

plasma levels of Glu and GOT enzymes did not differ statistically between *LAO1* KO and WT mice. However, T-Cho concentrations in *LAO1* KO mice were significantly lower ($P<0.05$) than those in control mice. GPT levels were significantly higher ($P<0.05$) in *LAO1* KO mice than in the WT mice (Fig. 1B).

Semi-quantitative RT-PCR analysis revealed that the expression of *PPAR-α*, *PPAR-γ*, and pro-inflammatory cytokine *IL-6* was not significantly high in *LAO1* KO mice (Fig. 1C). *TNF-α* levels were significantly higher ($P<0.05$) in KO mice than in the WT mice.

Gut microbiota composition

LAO1 mRNA and protein expression in the ileum and colon were analyzed using PCR and immunofluorescence, respectively. WT mice expressed LAO1 mRNA in the ileum and colon (Fig. 2). Furthermore, immunostaining revealed that the LAO1 protein was present on the surface of the ileum and colon epithelial cells of WT mice. Because WT mice express LAO1 in the gut, we further determined the differences in gut microbiota composition between WT and *LAO1* KO mice. Deep-sequence analysis revealed no differences in the microbiota composition between WT and *LAO1* KO mice, even at the α- and β-diversity levels (Fig. 3A and 3B, respectively). However, LDA size (LEfSe) was calculated to compare the composition of the gut microbiota between WT and *LAO1* KO mice, and it was found that *Mucispirillum* abundance was higher in WT mice. In contrary, the abundance of *Desulfovibrio* and *Muribaculaceae* was significantly higher ($P<0.01$) in *LAO1* KO mice (Fig. 3C).

SCFAs are the primary end-products of the gut microbiota. We found no significant differences in acetic and propionic acid levels between WT and *LAO1* KO mice (Fig. 3D).

We performed a gut permeability analysis to test gut leakage using FITC-dextran gavage and found no difference in the plasma levels of the chemicals between WT and *LAO1* KO mice (Fig. 3E).

FMT was performed in GF mice to investigate the potential relationship between liver gene expression and gut microbiota composition. Pro-inflammatory cytokine gene expression in the liver was examined four weeks after FMT. *TNF-α* and *IL-6* mRNA expression were not significantly higher than in *LAO1* KO mice compared to WT mice (Fig. 3F).

Metabolite levels in the portal and abdominal veins

The liver plays an essential role in detoxifying and neutralizing the metabolites produced throughout the body, particularly in the gut. We examined blood metabolites before (portal vein) and after entering the liver (abdominal vein). Differences in the metabolite

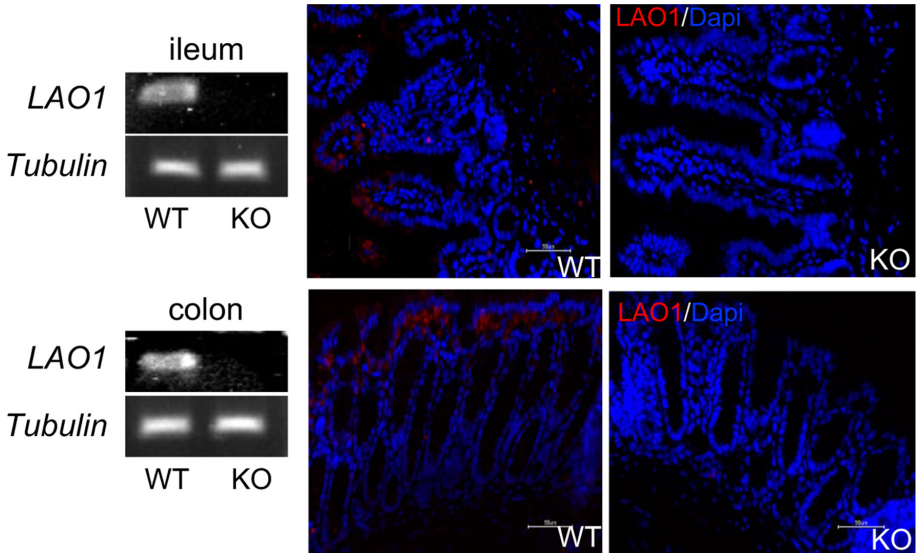

Fig. 2. L-amino acid oxidase-1 mRNA expression (left panel) and protein localization (right panel) in the ileum (upper pictures) and colon (lower pictures) of wild-type (WT) and *LAO1* KO mice.

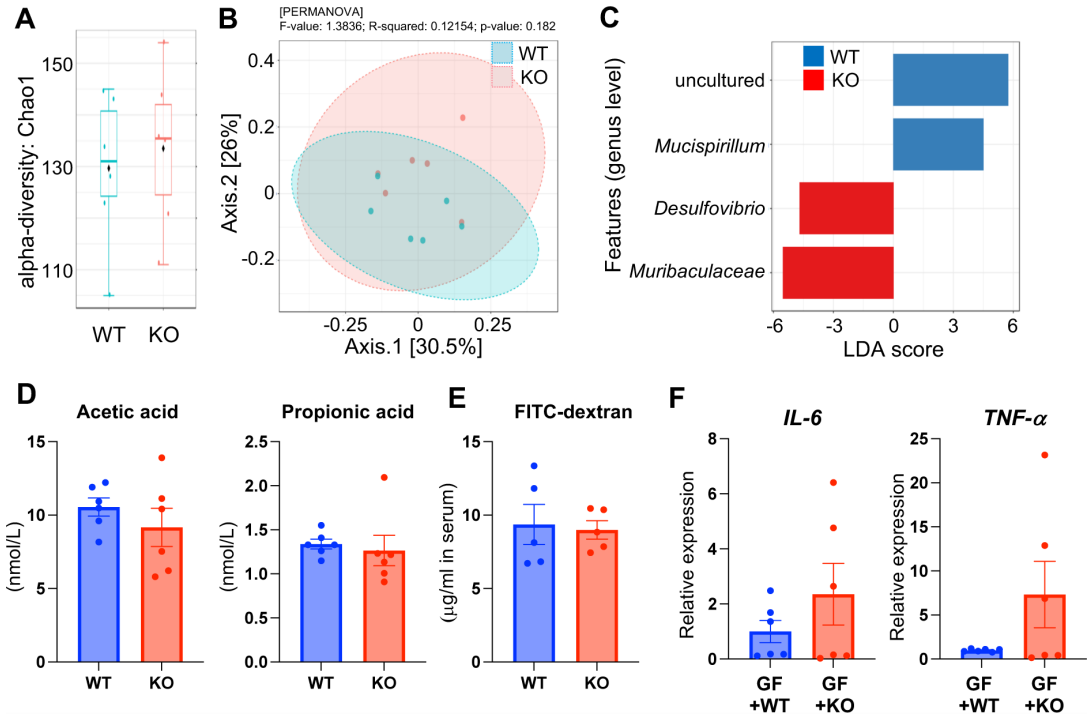

Fig. 3. Gut microbiota composition in wild-type (WT) and L-amino acid oxidase-1 knock-out (*LAO1* KO) mice. Alpha-diversity Chao1 richness box plot (**A**). Principal component analysis (PCoA) plots based on unweighted UniFrac distance matrices of microbial communities in WT and *LAO1* KO mice (**B**). Specific genera identified by linear discriminant analysis (LDA) effect size (LEfSe) in the feces of WT and *LAO1* KO mice (**C**). The concentration of acetic acid and propionic acid in the feces of WT and *LAO1* KO mice (**D**). The concentration of fluorescein isothiocyanate-conjugated dextran (FITC) (μg/mL) after four-hour administration of FITC-dextran in serum of wild-type (WT) and *LAO1* KO mice (**E**). Comparison of *interleukin-6* (left), and *tumor necrosis factor-α* (right) mRNA expression in the liver from germ-free (GF) mice transplanted with WT (GF+WT) and *LAO1* KO (GF+KO) mice feces (**F**).

content between the two veins were investigated using GC/MS metabolomic analysis. We observed different concentrations of various metabolites in both the portal (Fig. 4A) and abdominal veins (Fig. 4B). *LAO1* KO mice had significantly ($P<0.05$) higher 5-ALA, pyroglutamic acid, ethanolamine, and glyceric acid levels in the portal vein, and 5-ALA, D-Treitol, L-Sorbose, and pyruvic acid levels in the abdominal vein.

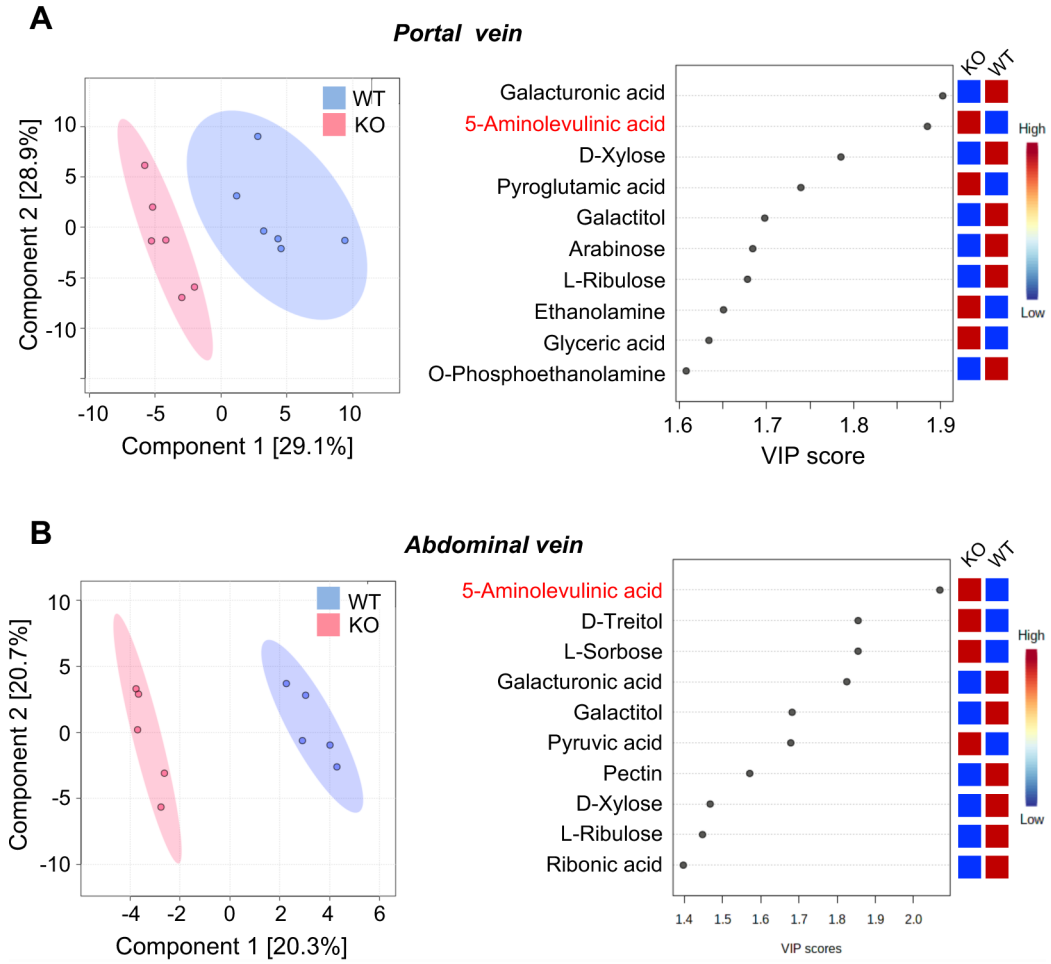

Fig. 4. Metabolite levels in the portal vein (**A**) and abdominal vein (**B**). 2D principal component analysis score plot of serum from wild-type (WT) and L-amino acid oxidase-1 knock-out (*LAO1* KO) mice (left panel). Important metabolites identified by partial least-squares discriminant analysis (right panel).

IP injection of 5-ALA

The high plasma 5-ALA levels in the two distinct blood circulations of *LAO1* KO mice, combined with the increased expression of pro-inflammatory cytokines in the liver, prompted us to inject higher doses of 5-ALA than biological concentrations into WT mice. Surprisingly, we discovered that IP injection of 100 mg/kg BW 5-ALA significantly ($P<0.05$) induced *IL-6* expression in the livers of WT mice (Fig. 5). However, *TNF-α* expression was not significantly different after IP injection of 5-ALA, at either low or high doses.

DISCUSSION

The gut microbiota contains a plethora of metabolites, hormones, and neurotransmitters that directly and indirectly modulate extraintestinal organs, such as the liver, brain, and kidneys [17]. Dysbiosis of the gut microbiota causes various liver diseases, including acute liver injury, non-alcoholic liver disease (NAFLD), and alcohol-related liver disease [22, 26]. The portal vein immediately exposes the liver to harmful substances produced by the gut microbiota because of a direct venous outflow from the gut. This study demonstrated that the absence of the *LAO1* gene increases pro-inflammatory cytokine expression in the liver by altering some plasma metabolites, including 5-ALA, and that the gut microbiome might partially contribute to these potential pathways. To the best of our knowledge, this is the first study to demonstrate the influence of gut microbiota on liver function in *LAO1* KO mice.

It has been reported that H_2O_2 produced by LAO1 is a critical component of antimicrobial activity in the mammary gland [18] and is most likely involved in the initial acquisition of gut microbiota in mice [23]. The findings of this study showed that the gut microbiota composition differed between WT and *LAO1* KO adult mice. *Mucispirillum* was more abundant in the feces of WT mice, whereas *Desulfovibrio* and *Muribaculaceae* were more abundant in the feces of *LAO1* KO mice. These results suggest that LAO1 present in the gut is essential for gut microbiota manipulation throughout life. In addition, FMT experiments revealed that GF mice transplanted with *LAO1* KO mouse feces had increased expression of *IL-6* and *TNF-α* in the liver. These observations suggested that LAO1 functions as a scavenger of harmful compounds and bacteria in the gut.

In this study, we found that the abundance of sulfur-reducing bacteria (*Desulfovibrio*) was higher in the feces of *LAO1* KO mice.

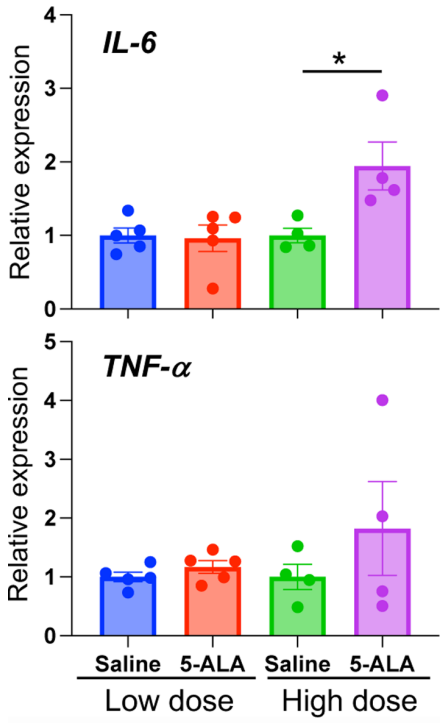

Fig. 5. Intraperitoneal injection of 5-aminolevulinic acid (5-ALA). Relative expression of inflammatory cytokines, such as *interleukin-6* and *tumor necrosis factor-α* mRNA, in wild-type (WT) mice liver after intraperitoneal (IP) injection of 5-ALA. Low dose: 40 mg/kg BW every day for one week. High dose: 100 mg/kg BW every three days for ten days.

Desulfovibrio is an anaerobic bacterium that is known to be the predominant sulfur-reducing bacterium in the human colon [6, 12]. *Desulfovibrio desulfuricans* (*D. desulfuricans*) was found in high concentrations in patients with ulcerative colitis and type 2 diabetes and has been linked to inflammatory bowel diseases, liver abscesses, and appendicitis [7, 25]. Recent studies have found that *D. desulfuricans* can increase intestinal permeability and the subsequent rise in lipopolysaccharide (LPS) transit from the intestine to the bloodstream. *D. desulfuricans* administration reduced the expression of ZO-1 and Occludin (proteins related to tight junctions in the intestinal barrier) in the colon of Apolipoprotein E KO mice. Furthermore, after treatment with the *D. desulfuricans* inoculation medium, the expression of two tight junction proteins in intestinal epithelial cells was inhibited [25]. These observations suggest that the increase in *Desulfovibrio* in *LAO1* KO mice might be associated with gut barrier disruption. However, we did not detect the high permeability of FITC-dextran in *LAO1* KO mice. Further studies are required to evaluate the gut barrier and investigate how sulfur-reducing bacteria increased in *LAO1* KO mice.

In *LAO1* KO mice, the GPT enzyme plasma level, associated with liver damage, was increased with higher expression of pro-inflammatory cytokines, such as IL-6 and TNF-α, in *LAO1* KO animal livers. Furthermore, 5-ALA concentrations in the portal and abdominal veins of *LAO1* KO mice were significantly higher than in the WT mice. 5-ALA is the first compound produced by the 5-ALA synthase in the heme biosynthetic pathway. To gain a better understanding, we injected 5-ALA into WT mice and found that a higher dose of this chemical significantly increased *IL-6* expression in the liver. We assumed that the high *IL-6* expression in the liver might indicate liver inflammation caused by 5-ALA administration. Previous human studies have revealed that 5-ALA administration as a photodynamic therapy agent reversibly increases the liver enzyme levels such as GPT, GOT, and alkaline phosphatase after surgery [16, 19, 20]. However, it has been reported that supplementation with 5-ALA as a food additive shows good performance in terms of iron transfer and anti-inflammatory and antioxidant properties in different animals, including fish [2], farm animals [10], and chickens [1]. These results indicate that the response of the body to 5-ALA may differ depending on the chemical dose and route of administration.

In conclusion, these findings suggest that *LAO1* is crucial for the regulation of gut microbiota composition and metabolite production in mice. In their absence, unusual bacteria may have a greater chance of thriving and altering liver activity via bacterial metabolites. However, there are conflicting findings on the benefits and risks of 5-ALA treatment. We discovered that administering a significant amount of 5-ALA to animals harms their liver function. Therefore, using 5-ALA in high doses as a therapeutic or feed additive should be considered.

CONFLICT OF INTEREST. The authors have no conflict of interest to disclose.

ACKNOWLEDGMENTS. The authors thank Mr. Ikki Mori for his valuable assistance with breeding and careful animal care.

REFERENCES

1. Chen J, Wang H, Wu Z, Gu H, Li C, Wang S, Liu G. 2022. Effects of 5-aminolevulinic acid on the inflammatory responses and antioxidative capacity in broiler chickens challenged with lipopolysaccharide. *Animal* **16**: 100575. [Medline] [CrossRef]
2. Cheng Y, Zhang J, Gao F, Xu Y, Wang C. 2022. Protective effects of 5-aminolevulinic acid against toxicity induced by alpha-cypermethrin to the liver-gut-microbiota axis in zebrafish. *Ecotoxicol Environ Saf* **234**: 113422. [Medline] [CrossRef]
3. Chong J, Wishart DS, Xia J. 2019. Using MetaboAnalyst 4.0 for comprehensive and integrative metabolomics data analysis. *Curr Protoc Bioinformatics* **68**: e86. [Medline] [CrossRef]
4. Chu H, Duan Y, Yang L, Schnabl B. 2019. Small metabolites, possible big changes: a microbiota-centered view of non-alcoholic fatty liver disease. *Gut* **68**: 359–370. [Medline] [CrossRef]
5. Compare D, Coccoli P, Rocco A, Nardone OM, De Maria S, Cartenì M, Nardone G. 2012. Gut--liver axis: the impact of gut microbiota on non alcoholic fatty liver disease. *Nutr Metab Cardiovasc Dis* **22**: 471–476. [Medline] [CrossRef]
6. Devereux R, He SH, Doyle CL, Orkland S, Stahl DA, LeGall J, Whitman WB. 1990. Diversity and origin of Desulfovibrio species: phylogenetic definition of a family. *J Bacteriol* **172**: 3609–3619. [Medline] [CrossRef]
7. Figueiredo MC, Lobo SA, Sousa SH, Pereira FP, Wall JD, Nobre LS, Saraiva LM. 2013. Hybrid cluster proteins and flavodiiron proteins afford protection to Desulfovibrio vulgaris upon macrophage infection. *J Bacteriol* **195**: 2684–2690. [Medline] [CrossRef]
8. Fujine K, Sano M, Katsumata Y, Sato K, Kobayashi E. 2021. Predicting the effective dose of 5-aminolevulinic acid to protect humans from renal ischemia-reperfusion injury: a study in micro miniature pigs. *J Cur Surg*. **11**: 8–14.
9. Hartmann P, Chu H, Duan Y, Schnabl B. 2019. Gut microbiota in liver disease: too much is harmful, nothing at all is not helpful either. *Am J Physiol Gastrointest Liver Physiol* **316**: G563–G573. [Medline] [CrossRef]
10. Hendawy AO, Khattab MS, Sugimura S, Sato K. 2020. Effects of 5-aminolevulinic acid as a supplement on animal performance, iron status, and immune response in farm animals: a review. *Animals (Basel)* **10**: 1352. [Medline] [CrossRef]
11. Hino H, Murayama Y, Nakanishi M, Inoue K, Nakajima M, Otsuji E. 2013. 5-Aminolevulinic acid-mediated photodynamic therapy using light-emitting diodes of different wavelengths in a mouse model of peritoneally disseminated gastric cancer. *J Surg Res* **185**: 119–126. [Medline] [CrossRef]
12. Hong Y, Sheng L, Zhong J, Tao X, Zhu W, Ma J, Yan J, Zhao A, Zheng X, Wu G, Li B, Han B, Ding K, Zheng N, Jia W, Li H. 2021. Desulfovibrio vulgaris, a potent acetic acid-producing bacterium, attenuates nonalcoholic fatty liver disease in mice. *Gut Microbes* **13**: 1–20. [Medline] [CrossRef]
13. Inoue R, Sakaue Y, Sawai C, Sawai T, Ozeki M, Romero-Pérez GA, Tsukahara T. 2016. A preliminary investigation on the relationship between gut microbiota and gene expressions in peripheral mononuclear cells of infants with autism spectrum disorders. *Biosci Biotechnol Biochem* **80**: 2450–2458. [Medline] [CrossRef]
14. Kasai K, Nakano M, Ohishi M, Nakamura T, Miura T. 2021. Antimicrobial properties of L-amino acid oxidase: biochemical features and biomedical applications. *Appl Microbiol Biotechnol* **105**: 4819–4832. [Medline] [CrossRef]
15. Kawase T, Hatanaka K, Kono M, Shirahase Y, Ochiai K, Takashiba S, Tsukahara T. 2020. Simultaneous determination of 7 short-chain fatty acids in human saliva by high-sensitivity gas chromatography-mass spectrometry. *Chromatogr* **41**: 63–71. [CrossRef]
16. Kim JH, Yoon HK, Lee HC, Park HP, Park CK, Dho YS, Hwang JW. 2019. Preoperative 5-aminolevulinic acid administration for brain tumor surgery is associated with an increase in postoperative liver enzymes: a retrospective cohort study. *Acta Neurochir (Wien)* **161**: 2289–2298. [Medline] [CrossRef]
17. Milosevic I, Vujovic A, Barac A, Djelic M, Korac M, Radovanovic Spurnic A, Gmizic I, Stevanovic O, Djordjevic V, Lekic N, Russo E, Amedei A. 2019. Gut-liver axis, gut microbiota, and its modulation in the management of liver diseases: a review of the literature. *Int J Mol Sci* **20**: 395. [Medline] [CrossRef]
18. Nagaoka K, Aoki F, Hayashi M, Muroi Y, Sakurai T, Itoh K, Ikawa M, Okabe M, Imakawa K, Sakai S. 2009. L-amino acid oxidase plays a crucial role in host defense in the mammary glands. *FASEB J* **23**: 2514–2520. [Medline] [CrossRef]
19. Offersen CM, Skjoeth-Rasmussen J. 2017. Evaluation of the risk of liver damage from the use of 5-aminolevulinic acid for intra-operative identification and resection in patients with malignant gliomas. *Acta Neurochir (Wien)* **159**: 145–150. [Medline] [CrossRef]
20. Oh H, Park JB, Yoon HK, Lee HC, Park CK, Park HP. 2020. Effects of preoperative 5-aminolevulinic acid administration on postoperative liver enzymes after brain tumor surgery in patients with elevated preoperative liver enzymes. *J Clin Neurosci* **72**: 304–309. [Medline] [CrossRef]
21. Puiffe ML, Lachaise I, Molinier-Frenkel V, Castellano F. 2013. Antibacterial properties of the mammalian L-amino acid oxidase IL4I1. *PLoS One* **8**: e54589. [Medline] [CrossRef]
22. Quigley EMM, Stanton C, Murphy EF. 2013. The gut microbiota and the liver. Pathophysiological and clinical implications. *J Hepatol* **58**: 1020–1027. [Medline] [CrossRef]
23. Shigeno Y, Zhang H, Banno T, Usuda K, Nochi T, Inoue R, Watanabe G, Jin W, Benno Y, Nagaoka K. 2019. Gut microbiota development in mice is affected by hydrogen peroxide produced from amino acid metabolism during lactation. *FASEB J* **33**: 3343–3352. [Medline] [CrossRef]
24. Usuda K, Kawase T, Shigeno Y, Fukuzawa S, Fujii K, Zhang H, Tsukahara T, Tomonaga S, Watanabe G, Jin W, Nagaoka K. 2018. Hippocampal metabolism of amino acids by L-amino acid oxidase is involved in fear learning and memory. *Sci Rep* **8**: 11073. [Medline] [CrossRef]
25. Zhang K, Qin X, Qiu J, Sun T, Qu K, Din AU, Yan W, Li T, Chen Y, Gu W, Rao X. 2023. Desulfovibrio desulfuricans aggravates atherosclerosis by enhancing intestinal permeability and endothelial TLR4/NF-κB pathway in Apoe−/−mice. *Genes Dis* 10: 239–253. [Medline]
26. Zheng Z, Wang B. 2021. The gut-liver Axis in health and disease: the role of gut microbiota-derived signals in liver injury and regeneration. *Front Immunol* **12**: 775526. [Medline] [CrossRef]